CO adsorption on Cu-Pd alloy surfaces: ligand versus ensemble effects

Sung Sakong*, Christian Mosch, and Axel Groß
Institut für Theoretische Chemie, Universität Ulm, Albert-Einstein-Allee 11, 89069 Ulm/Germany
(Dated: October 25, 2006)

The CO adsorption on ordered Cu-Pd alloy surfaces and surface alloys has been studied using density functional theory (DFT) within the framework of the generalized gradient approximation (GGA). On the surface alloys, the CO adsorption energy at the top sites decreases with increasing concentration of the more reactive metal Pd. This surprising ligand effect is caused by the effective compressive strain induced by the larger Pd atoms. On the other hand, at the most favorable adsorption sites the CO binding becomes stronger with increasing Pd concentration which is caused by an ensemble effect related to the availability of higher coordinated adsorption sites. At the surfaces of the bulk alloys, the trends in the adsorption energy as a function of the Pd concentration are less clear because of the strong Pd-Cu interaction and the absence of effective strain effects.

I. INTRODUCTION

Commercial catalysts often consist of metal alloys which exhibit a superior performance compared to the single constituents. Therefore, the manipulation of the properties of catalysts by alloying is of significant importance in catalyst research [1–3]. A deeper understanding of the underlying electronic and geometric factors that determine the catalytic properties of alloys can thus be very beneficial for the rational improvement of catalysts [4–8]. For that purpose, ordered bimetallic surfaces are particularly well-suited. On the one hand, they are simple enough for a systematic study of the relationship between microscopic structure and catalytic activity. On the other hand, they offer a broad variety of possible structures and compositions with a significant degree of complexity.

The composition and the intermetallic interaction in a bimetallic system have a strong influence on its catalytic properties. These effects are often discussed within the concept of the *ligand* versus the *ensemble* effect [1]. The term ligand effect refers to the modifications in the catalytic activity and selectivity caused by the electronic interaction between the components of a bimetallic system. On the other hand, for many reactions, a certain number of active sites is required. By blocking a large ensemble of active sites, these reactions can be suppressed thus increasing the selectivity towards reactions that only need a small ensemble of active sites. This is called the ensemble effect. In addition to these effects, the modification of the interatomic distances in a bimetallic system can have a decisive influence on its catalytic activity [9]. This *geometric effect* should also be considered together with the ensemble and ligand effects when the reactivity of bimetallic systems is discussed.

The adsorption of carbon monoxide on bimetallic systems has been extensively studied as a model system both experimentally [1, 2, 10–14] and theoretically [3, 8, 9, 15–22], since this is the first step towards more complex processes like methanol synthesis, reduction of CO and reactions in direct methanol fuel cells. PdCu alloys are in particular of interest as a catalyst for the CO oxidation by NO [10, 11, 23]. In addition, the hydrogen permeability of Cu-Pd membranes make this material interesting for the design of efficient hydrogen filters in industry [24, 25].

Recently, temperature-programmed desorption (TPD) experiments of the CO interaction with ultra-thin Cu-Pd alloys deposited on a Ru(0001) substrate were performed by Hager *et al.* [14]. The CO binding energy on a Pd monolayer on the Ru substrate turned out to be smaller than the binding energy on pure Pd. In contrast, the binding energy on a Cu monolayer is larger than on pure Cu. This behaviour can be understood within the context of the d-band model, which was proposed by Hammer and Nørskov [26, 27]. For pseudomorphic overlayers, their lateral lattice constant is adjusted to the underlying Ru substrate, In the case of Pd/Ru, this leads to a compressed overlayer while Cu/Ru is expanded. An expansion of the lattice causes an d-band upshift which is related to a stronger interaction with adsorbates according to the d-band model whereas in the case of a compression the induced d-band downshift causes smaller adsorption energies. Strain effects have also been used in order to explain the adsorption properties in surface alloys as a function of the alloy composition [16, 17, 19].

The CO adsorption on CuPd and Cu_3Pd bulk alloys and a substitutional Pd/Cu(111) surface alloy has been addressed theoretical studies [18, 28] based on density functional theory (DFT). The calculations confirmed the important influence of both strain effects and the electronic interaction between the two components of a bimetallic surface on its chemical properties. Furthermore, DFT calculations of the hydrogen adsorption on Pd/Cu and Cu/Pd pseudomorphic overlayers carried out in our group [29] showed that these overlayers exhibit intermediate properties between those of the pure Pd and Cu surfaces because of the strong Pd-Cu interaction which also favors the formation of PdCu alloys.

In the following, we will present one of the first systematic theoretical studies of the adsorption on bimetallic substrates addressing bulk alloys, pseudomorphic over-

*New address: Fachbereich Physik, Universität Duisburg-Essen, Lotharstraße 1, 47048 Duisburg/Germany

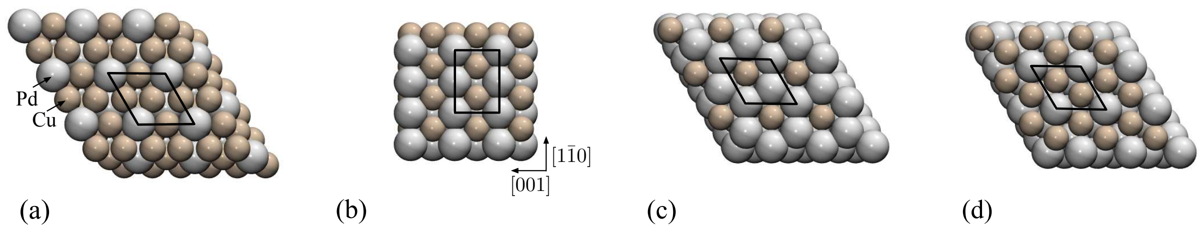

FIG. 1: Illustration of the bimetallic surface structures addressed in this study including the used surface unit cells for CO adsorption. a) $Cu_3Pd(111)$ b) CuPd(110), c) $CuPd_2/Pd(111)$, d) $Cu_2Pd/Pd(111)$.

layers and surface alloys, using CO as the probe molecule. Realistic bimetallic systems often do not consist of pure pseudomorphic overlayer, as often investigated in surface science studies, but rather form bulk or surface alloys. By addressing the CO adsorption at these complex alloy structures, we are trying to contribute to closing the materials gap between surface science and heterogeneous catalysis.

This paper is structured as follows. After describing the theoretical bachground of the calculations, the CO adsorption on pure Cu and Pd surfaces will be covered in Sec. III A. Escpecially the effects of various exchange-correlation functionals will be discussed in this section in order to find a proper description of the CO adsorption on bimetallic substrates. In Sec. III B and Sec. III C, the properties of the CO adsorption on bulk alloy surfaces and pseudomorphic overlayers are analysed. Finally, we will discuss the relation between alloying and reactivity of the surface in terms of the electronic structure.

II. THEORETICAL BACKGROUND

Density functional theory calculations have been performed using the Vienna *ab initio* simulation package (VASP) [30]. Exchange-correlation effects are described within the generalized gradient approximation (GGA). The accuracy of the considered functionals, PW91 [31], PBE [32] and RPBE [33], is checked for several adsorption sites of CO on Cu(111) (see the next section). Based on these findings, the RPBE functional is used for the bimetallic systems. The ionic cores are represented by the projector augmented wave (PAW) method [34, 35]. The wave function is represented by a plane wave basis set with an energy cutoff of 400 eV.

The substrate is described by a five layer slab. In the case of bulk alloy surfaces, the two uppermost layers are fully relaxed whereas for pseudomorphic overlayers on alloy surfaces, the overlayer is fully relaxed together with the two underlying substrate layers. A rather fine Monkhorst-Pack mesh of $15 \times 15 \times 1$ **k**-points is used to achieve an accurate description of the density of states near the Fermi level. A $(\sqrt{3} \times \sqrt{3})$R30° adsorption structure is selected for pure Cu and Pd and the pseudomorphic overlayer systems. For $Cu_3Pd(111)$ and CuPd(110), the CO adsorption in (2×2) and (2×1) surface unit cells has been considered, respectively. The structure of the surfaces and the corresponding surface unit cells are illustrated in Fig. 1.

The vibrational frequencies of CO on the various bimetallic surfaces are obtained by fixing the geometric center of the CO molecule, expanding the C-O bond along the bond axis, calculating the total energy of the system for different CO-distances and finally fitting these energies to a Morse potential. The calculated RPBE-DFT binding energy and the vibrational frequency of CO in gas-phase are 11.19 eV and 2143 cm^{-1}. This is in satisfactory agreement with the experimental values of 11.24 eV and 2170 cm^{-1} [36].

Experimentally, chemisorbed CO is mostly found on the ontop sites of Pt and Cu surfaces [37–42] while in DFT calculations using local or semi-local funtionals the fcc-hollow site is energetically most favorable [43]. This discrepancy between theory and experiment is caused by the overestimation of the back-donation into the $2\pi^*$ orbital of CO which is mainly caused by the fact that the HOMO-LUMO gap is too small in most of the semi-local DFT exchange-correlation functionals. In this case, the $2\pi^*$ orbital interacts stronger with the surface electrons at the hollow site than at the top site [44]. As a result, the hollow site becomes energetically more stable than the top site. As a first approach to remedy this problem, more repulsive exchange-correlation functionals have been tried [18, 44, 45]. However, the most remarkable progress has been obtained by an sophisticated application of the GGA+U method [46–48]. In these studies, a constraint in the occupancies of the CO molecular orbitals leads to a dramatic improvement compared to Dudarev's conventional LDA+U-approach [49]. The larger HOMO-LUMO gap results in an appropriate description of the adsorption site and a more accurate binding strength of CO on the metal surface. In spite of the success of the GGA+U approach, it is still questionable if one can apply it to an alloy system. In order to describe the correlation effects, only one empirically selected U parameter is chosen in the GGA+U approach, and in general such a parameter will not be appropriate for both alloy elements simultaneously. Since the description of CO adsorption on Pd surfaces is already successful in conventional DFT, and since the combined contribution of Cu-Pd hybrids to CO adsorption is unclear, we will stay within the semilocal DFT (GGA) framework rejecting any empirical parameter in this work.

III. RESULTS

A. CO adsorption on pure metal surfaces

The experimental heat of adsorption of CO on pure Cu(111) is in the range of 0.44 to 0.52 eV [39–42]. The experimentally measured adsorption position is the top site. Hollow site adsorption is only observed for higher CO coverages. As Table I shows, the RPBE functional reproduces the experimental CO binding energy on the top site quantitatively. In contrast, the PBE and PW91 functionals overestimate the binding strength by more than 0.2 eV. These binding energies are slightly larger compared to a previous study [18], probably due to the different treatment of the ion cores. However, all three functionals erroneously predict the hollow site as the most favorable site, however, the RPBE functional yields the smallest difference in the adsorption energies between top and fcc hollow sites. The adsorption height on the top position is measured to be 1.91 Å by Moler *et al.* [50], which is in good agreement with the results of all considered DFT-GGA functionals.

On Pd(111), the most favorable adsorption site is the fcc hollow site at a coverage of $\theta = 1/3$ according to both experiment [51, 52] and theory [53]. The desorption energy is measured to be 1.24 eV by TPD experiments [54], the stretch frequency is 1849 cm^{-1} according to IR spectroscopy experiments [54, 55]. At the adsorption position, the CO molecule is located 1.27 Å above the surface with a bond length of 1.14 Å [52]. The calculated adsorption geometry (see Table I) is in good agreement with the experiment, but the adsorption energy at the fcc hollow site is overestimated in the PW91 and RPBE calculations by about 0.75 eV and 0.4 eV, respectively. For a very low coverage the experimental CO binding energy is increased to 1.54 eV due to the reduced repulsive interaction between the CO molecules, however, this experimental value is still smaller than the theoretical values for a coverage of $\theta = 1/3$. An analysis of the electronic structure yields that the population of the Pd d-electrons is reduced by a 4d→5s5p hybridization which weakens the back-donation into the $2\pi^*$ orbital [1]. However, in the DFT-GGA calculations, the low-lying oxygen p-state takes part in the CO-Pd interaction and leads to an additional back-donation effect which makes the CO-metal bonding too attractive.

Surfaces	V_{xc}		E_{ads} (eV)	h_{M-C} (Å)	d_{M-C} (Å)	d_{CO} (Å)	ν_{CO} (cm^{-1})
Cu(111)	PW91	top	−0.74	1.86	1.86	1.16	2008
		fcc	−0.85	1.41	2.04	1.18	
		hcp	−0.86	1.42	2.05	1.18	
		bridge	−0.78	1.50	1.98	1.17	
	PBE	top	−0.72	1.86	1.86	1.16	
		fcc	−0.84	1.40	2.04	1.18	
		hcp	−0.85	1.41	2.04	1.18	
		bridge	−0.77	1.50	1.98	1.18	
	RPBE	top	−0.47	1.88	1.88	1.16	2003
		fcc	−0.50	1.43	2.07	1.18	1848
		hcp	−0.50	1.43	2.07	1.18	1885
		bridge	−0.44	1.52	2.00	1.18	1861
Pd(111)	PW91	top	−1.42	1.87	1.87	1.16	
		fcc	−1.99	1.30	2.07	1.19	
		hcp	−1.97	1.31	2.07	1.19	
	RPBE	top	−1.14	1.88	1.88	1.16	2016
		fcc	−1.65	1.30	2.08	1.19	1792
		hcp	−1.63	1.31	2.08	1.19	1793
		bridge	−1.48	1.44	2.01	1.18	1864

TABLE I: CO adsorption properties on pure Cu(111) and Pd(111) for various exchange-correlation functionals. A negative adsorption energy E_{ads} means attraction. h_{M-C} is the height of C above the first surface layer. d_{M-C} is the distance of C to the nearest surface atom. d_{CO} is the equilibrium distance of C and O, ν_{CO} is the vibrational frequency of the CO molecule. In case of Cu(111), all exchange-correlation functions result in a wrong prediction of the hollow sites to be more stable than the top site. However in case of RPBE the miss is rather narrow.

According to IR experiments, the CO stretch frequency at the top site of Cu(111) is 2078 cm^{-1} corresponding to a redshift from the gas-phase value by about 90 cm^{-1} [39]. In contrast, DFT calculations using the PW91 and RPBE functionals yield a redshift of 140 cm^{-1} (see Table I)). On Pd(111) the experimental stretch frequency is redshifted by 321 cm^{-1} and 73 cm^{-1} at the fcc and top sites, respectively [54, 55] which should be compared to the DFT results of 351 cm^{-1} and 127 cm^{-1} for the redshifts. Thus the DFT calculation systematically overestimate the redshift of the CO stretch frequency upon adsorption on Cu and Pd. This can be understood by the unrealistically strong back-donation into the $2\pi^*$ orbital which weakens the CO bonding and decreases its stretch frequency [56]. Interestingly, Kresse's GGA+U approach does not change the ground state configuration but moderates the amount of the redshift of the CO stretch frequency compared to conventional GGA-DFT calculations [46, 47]. This demonstrates the effect of the larger HOMO-LUMO gap that decreases the back-donation and leads to a smaller redshift of the stretch frequency. Furthermore, taking into account the coupling of the stretch vibrations to the substrate atoms via a first-order mass correction reduces the redshifts by about to 20 cm^{-1} [57] which would lead to a much better agreement with the experiment.

Interestingly, the CO stretch frequencies on the fcc and hcp threefold hollow sites of Cu(111) differ by 37 cm^{-1} in spite of practically the same CO adsorption energies whereas on Pd(111) the CO stretch frequencies on the two threefold hollow sites are very similar. Apparently, on Cu(111) there is a much stronger interaction of the CO with the second-layer atom below the CO molecule at the hcp site than on Pd. This is reflected in a much stronger relaxation of 0.1 Å of the second-layer Cu atom below the hcp site upon CO adsorption compared to 0.02 Å for Pd.

The results presented in this section show that the RPBE functional yields the best description of the properties of the CO molecule. Therefore all further calculations presented in this study have been obtained with the RPBE functional. Still, the adsorption energies at bridge and hollow sites of PdCu alloys might be overestimated. Furthermore, the site preference at sites involving Cu atoms might not be correct since it is not correctly reproduced for pure Cu(111). However, in this study we are mainly interested in trends in the adsorption energy as a function of the composition of bimetallic PdCu surfaces, and these trends should be reliable be given by the DFT-GGA calculations.

B. CO adsorption on bulk crystal alloys

Two PdCu alloys with different composition are considered in this study, Cu_3Pd and CuPd. The Cu_3Pd alloy is an fcc crystal of $L1_2$ symmetry, whereas CuPd is an bcc alloy of B_2 symmetry. For both alloys, the most densely packed surface terminations have been selected, $Cu_3Pd(111)$ and CuPd(110), which both maintain the bulk stoichiometry at the surface. Thus the determination of the chemical properties of both alloy constituents is possible. The CO coverage corresponds to one molecule per four surface atoms which we denote as $\theta = 1/4$.

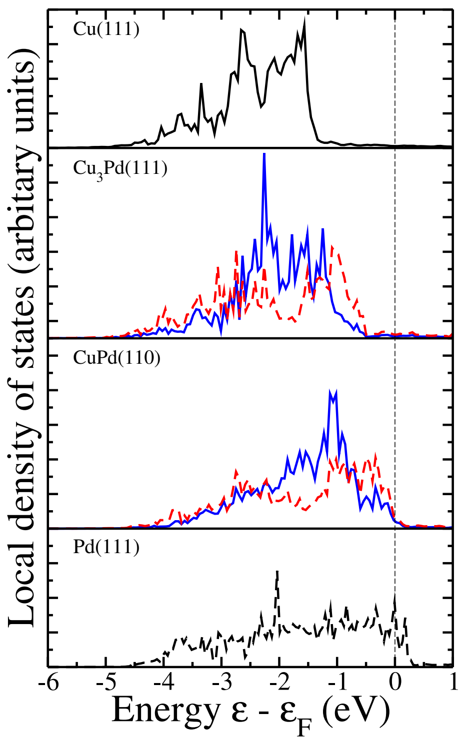

FIG. 2: Local d-band density of states of $Cu_3Pd(111)$ and CuPd(110) bulk alloy surfaces compared to clean Cu(111) and Pd(111). The Cu d-states are represented by solid lines, the Pd states by dashed-lines.

The d-band local density of states (LDOS) of the bulk alloy surfaces is plotted in Fig. 2 in comparison with those of clean Cu and Pd surfaces. The strong Cu-Pd interaction leads to a significant hybridization of the Pd and Cu orbitals. The Pd d-band density is considerably reduced at the Fermi level and nearly vanishes there, which is more pronounced for $Cu_3Pd(111)$ than for CuPd(110). The Cu d-band is shifted upwards towards the Fermi level. Such a behavior is commonly found in noble metal Pd-alloys [58–61]. Experimentally, a certain amount of electron transfers from Pd to Cu is furthermore infered [58, 60, 62].

The CO adsorption properties on Cu-Pd bulk alloy surfaces are listed in Table II. The binding energies on $Cu_3Pd(111)$ are in good agreement with previous DFT-RPBE results by Lopez and Nørskov [18]. In contrast to the prediction of the d-band model, the adsorption energy on the top position of Cu in Cu(111), $Cu_3Pd(111)$ and CuPd(110), is to a large extend independent of the position of the d-band center (see also Fig. 5). Such a failure of the d-band model has also been found in DFT calculations of hydrogen adsorption on defect-rich Cu surfaces [63] and strained Cu surface [64]. In contrast to our results for the CuPd(110) surface, previous DFT calculations demonstrate that the adsorption energy on CuPd(111) is 0.5 eV larger than on pure Cu [18]. CuPd(111) is a highly open surface, thus the adsorption properties on the surface cannot be directly compared to the results of close packed surfaces. As far as the Pd top sites are concerned, the CO adsorption energy is reduced by 0.1 eV on CuPd(110) and by 0.3 eV on $Cu_3Pd(111)$ compared to pure Pd(111), now in agreement with the predictions of the d-band model. In fact, a reduced CO adsorption energy at the Pd top sites is expected for all bulk alloy surfaces containing Pd, since Pd atoms have a more noble metal-like d-structures in bulk alloys.

The adsorption energy difference between top and hollow sites for alloy surfaces tends to be smaller than for pure surfaces. On $Cu_3Pd(111)$ the favorable adsorption sites are located atop of the isolated Pd atoms and its surrounding hollow sites while the area around the Cu atoms is less favorable. CuPd(110), on the other hand, consists of Cu and Pd rows running in the $[\bar{1}10]$ direction with the Pd rows more reactive for CO adsorption.

The adsorption energy of bulk Cu-Pd alloys shows an intermediate behaviour between pure Cu and pure Pd, as has already been found for PdCu overlayer systems [29]. This behavour is not found in case of Pt-Ru alloys [19, 20]. There, both strain effects as well as the strong interaction between Pt and Ru lead to an even weaker binding on Pt and an even stronger binding on Ru, compared to the pure metals. The Pt-Ru interaction is weaker than Ru-Ru and stronger than Pt-Pt interaction, thus Ru-CO binding becomes stronger in the presence of neighboring Pt atoms [9]. In addition, the more reactive metal (Ru) has a smaller lattice constant than the less reactive (Pt). In contrast, for Cu-Pd sys-

Surface	Adsorption position	E_{ads} (eV)	h_{Pd-C} (Å)	d_{Pd-C} (Å)	h_{Cu-C} (Å)	d_{Cu-C} (Å)	d_{CO} (Å)	ν_{CO} (cm^{-1})
$Cu_3Pd(111)$	top_{Pd}	−0.90	1.93	1.93			1.16	2005
	top_{Cu}	−0.41			1.87	1.87	1.16	
	fcc_{Cu_2Pd}	−0.72	1.44	2.02	1.48	2.19	1.18	
	hcp_{Cu_2Pd}	−0.77	1.38	2.10	1.40	2.10	1.18	
	fcc_{Cu_3}	−0.58			1.36	2.04	1.18	1841
	hcp_{Cu_3}	−0.21			1.40	2.10	1.18	1828
CuPd(110)	top_{Pd}	−1.11	1.90	1.90			1.16	2010
	top_{Cu}	−0.50			1.84	1.84	1.16	1994
	$bridge_{Cu_2}$	−0.81	1.67	2.44	1.26	2.01	1.19	1776
	$bridge_{Pd_2}$	−1.32	1.42	2.05	1.45	2.58	1.18	1775
Pd/CuPd(110)	top_{Pd}	−1.04	1.88	1.88			1.16	
	fcc_{Pd_3}	−1.52	1.21	2.09			1.19	
	$bridge_{Pd_2}$	−1.38	1.37	2.02			1.18	

TABLE II: Properties of CO molecules adsorbed on the close packed Cu-Pd alloy surfaces. The adsorption configuration is labeled by the adsorption position, e.g. fcc, and the nearest surface atoms, e.g. $_{Cu_2Pd}$. The vibrational frequency of CO is only evaluated for the molecules in an upright configuration.

tems the more reactive metal (Pd) has a *larger* lattice constant than the less reactive (Cu). Therefore, the geometric strain effect and the strong ligand effect result in opposing trends [9] leading to intermediate chemical properties.

When an alloy surface is considered, segregation becomes an important issue. At the surface, the stoichiometry can be different from the alloy bulk stoichiometry. In fact, a strong adsorbate induced Pd segregation has been observed on CuPd(110) [65]. In order to address the effects of this adsorbate induced surface segregation, we have also considered CO adsorption on a Pd monolayer on CuPd(110). Pd forms a buckled overlayer on CuPd(110) with a corrugation amplitude in the different heights of 0.4 Å, however, if CO adsorbs on fcc site, the Pd overlayer becomes smoother. The binding strength of CO on Pd/CuPd(110) is 0.2 eV larger than on CuPd(110), providing a driving force for the experimentally observed adsorbate induced surface segregation. As the comparison of the CO adsorption energies on the three different surfaces considered in Table II demonstrates, the most favorable adsorption site changes from fcc_{Pd_3} to top_{Pd} with decreasing Pd density.

It has been demonstrated by IR spectroscopy experiments in which peaks assigned to the hollow site are decreasing on supported Cu-Pd catalysts, while the peak assigned to top site is increasing [10]. The vibrational frequencies are increased on both, Cu and Pd top sites with increasing CO density [14].

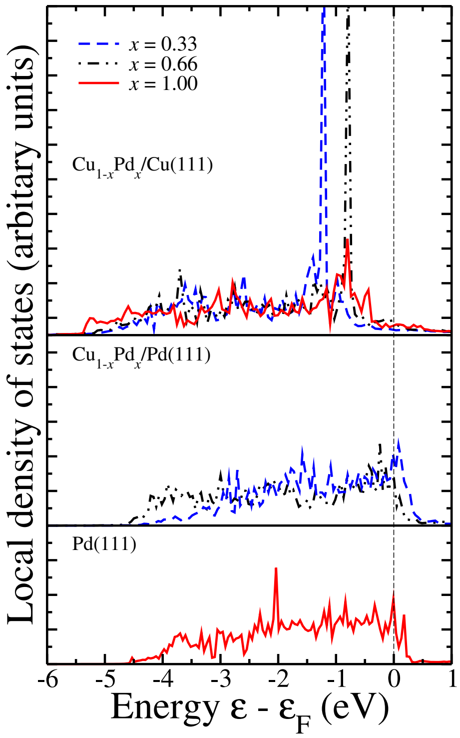

FIG. 3: The Pd d-band local density of states of monolayer alloys on Cu(111) (upper panel) and on Pd(111) (middle panel) for various Pd concentrations compared with the LDOS of pure Pd(111) (lower panel). The Pd d-band width increases with increasing Pd content. On Cu, the Pd bands are shifted to lower energies caused by the 8% suppression.

C. CO adsorption on overlayer systems

We will now turn to pseudomorphic Pd and Cu monolayers and Cu-Pd surface alloys on both Cu(111) and Pd(111). In these overlayer systems, thin films are created with the lateral lattice constants of Cu and Pd, respectively. For the surface alloys, the Pd concentration has been selected to be 1/3 and 2/3. These surface alloys can be interpreted as isolated Pd or Cu atoms with an coverage of 1/3 in a surface matrix of the other metal (see Fig. 1). Not all of these surface alloy structures are necessarily thermodynamically stable, considering the large lattice mismatch of 8% between Pd and Cu. For example, because of the strong compression by 8%, a Pd overlayer on Cu is not stable [9, 18, 66]. However, performing a systematic study of the CO adsorption energy on these different overlayer systems will reveal the importance of geometric strain effects compared to the electronic ligand effects of the Cu-Pd interaction. Furthermore, at the surface alloys, adsorbates can not necessarily find sites that are highly coordinated with respect to the more active metal. Thus we will also be able to assess the role of the ensemble effect.

The Pd d-band LDOS of the monolayer surface alloys for various Pd concentrations are plotted in Fig. 3. On the Cu substrate (upper panel), the Pd d-bands are broadened and located at significantly lower energies than on the Pd substrate (middle panel). This is caused by the 8% suppression: the suppression increases the overlap between the Pd orbitals which makes the bands broader and thus reduces the number of occupied d-states in a not completely, but more than half filled d-band. When there is no significant charge transfer, then the d-band has to shift down in order to preserve the degree of d-band filling [67]. As Fig. 3 shows, on Cu(111) the number of unoccupied Pd d-states is reduced compared to Pd(111). Still, the upper edge of the Pd d-band intersects with the Fermi level in all considered monolayer alloys, demonstrating that Pd maintains its transition metal characteristics in thin surface alloys.

The adsorption properties of CO on the monolayer alloys are listed in Table III. As far as the pure overlayer systems are concerned, the Cu and Pd monolayers lying on the other metal substrate represent expanded and compressed layers, respectively. On the expanded Cu layer, the binding energy of CO is increased by 0.3 eV compared to pure Cu(111), while on the compressed Pd layer the CO-Pd interaction is reduced by 0.6 eV. These changes of the CO adsorption energies are about twice as large as the corresponding shifts in the atomic hydrogen adsorption energies on the same substrates [29].

The CO adsorption energies at the top sites of Pd and Cu on various alloy surfaces and at the most favorable sites are plotted in Fig. 4 as a function of the Pd concentration. The most striking result is that the trend of the adsorption energies at the top sites (4a) is exactly opposite to the one at the most favorable sites (4b): At the top sites of the surface alloys, the adsorption energies rises approximately linearly with increasing Pd concentration, i.e., the binding becomes weaker, while at the most favorable sites the binding becomes stronger with increasing Pd concentration. These results can be summarized by saying that obviously the reactivity of the single Pd and Cu atoms decreases for larger Pd concentrations whereas the overall reactivity of the whole surface alloy increases.

These findings are at first sight surprising since the CO binding to the top sites decreases with the increasing concentration of the more reactive metal, Pd. It is well known that strain in surface layers can significantly modify adsorption energies [27, 64, 68]. In surface alloys, a growing concentration of the larger element effectively corresponds to the introduction of compressive strain which then reduces the reactivity of the surface. Such a dependence has also been found in previous DFT calculations for Au-Pd alloy surfaces [17] and for Pt-Ru alloy surfaces [16, 19]. As Fig. 4a shows, the effective strain effects are larger on Cu(111) where the binding energy is decreased by 0.3 eV at the top sites when the Pd concentration is increased by 2/3 whereas this decrease amounts to only 0.2 eV on Pd(111). This can be understood considering the fact that the local compression is effectively stronger on Cu substrate whose lateral

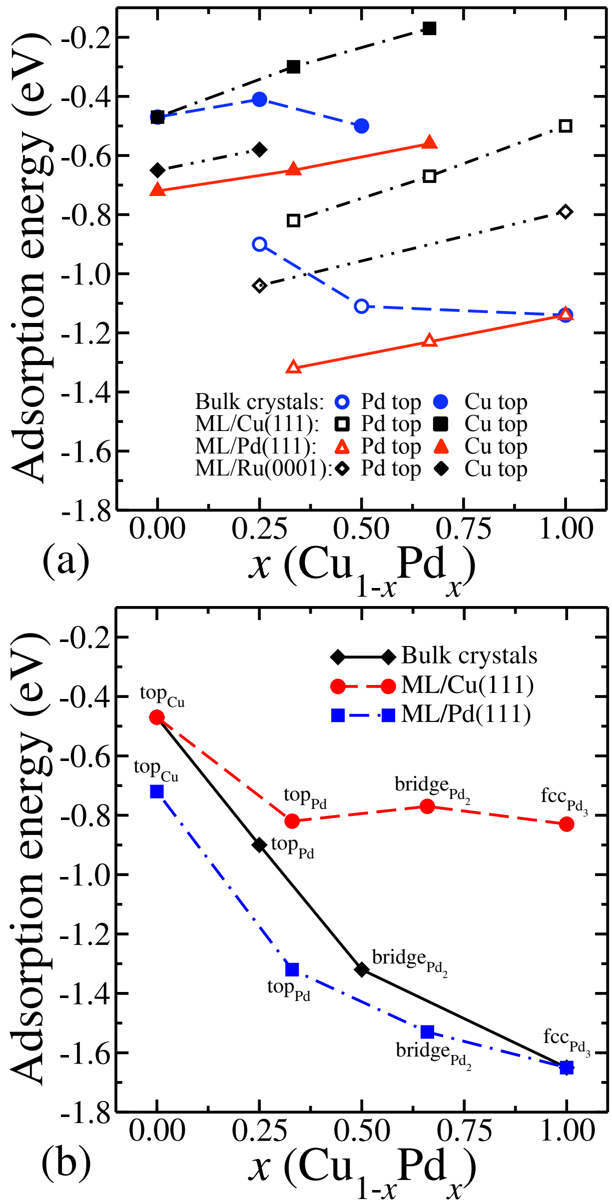

FIG. 4: CO adsorption energies as a function of the Pd concentration x on various alloy surfaces at the top sites of Pd and Cu (a) and at the most favorable sites (b).

Underlying Substrate	x ($Cu_{1-x}Pd_x$)		E_{ads} (eV)	h_{Pd-C} (Å)	d_{Pd-C} (Å)	h_{Cu-C} (Å)	d_{Cu-C} (Å)	d_{CO} (Å)	ν_{CO} (cm^{-1})
Cu(111)	0.33	top_{Pd}	−0.82	1.93	1.93			1.16	2011
		top_{Cu}	−0.30			1.89	1.89	1.16	1996
		fcc_{Cu_2Pd}	−0.62	1.44	2.03	1.55	2.17	1.18	
		hcp_{Cu_2Pd}	−0.61	1.43	2.04	1.53	2.15	1.18	
	0.66	top_{Pd}	−0.67	1.92	1.92			1.16	2012
		top_{Cu}	−0.17			1.90	1.90	1.15	2064
		$bridge_{Pd_2}$	−0.77	1.58	2.04	1.88	2.90	1.17	
	1.00	top_{Pd}	−0.50	1.91	1.91			1.16	2008
		fcc_{Pd_3}	−0.83	1.46	2.10			1.18	1865
		hcp_{Pd_3}	−0.82	1.46	2.10			1.18	1865
Pd(111)	0.00	top_{Cu}	−0.72			1.85	1.85	1.16	2003
		fcc_{Cu_3}	−0.71			1.35	2.07	1.18	1843
		hcp_{Cu_3}	−0.72			1.38	2.06	1.18	
	0.33	top_{Pd}	−1.32	1.89	1.89			1.16	2018
		top_{Cu}	−0.65			1.85	1.85	1.16	2000
		fcc_{Cu_2Pd}	−1.14	1.28	2.00	1.43	2.15	1.18	
		hcp_{Cu_2Pd}	−1.11	1.30	2.01	1.45	2.13	1.18	
	0.66	top_{Pd}	−1.23	1.88	1.88			1.16	2018
		top_{Cu}	−0.56			1.85	1.85	1.16	1998
		$bridge_{Pd_2}$	−1.53	1.41	2.02	1.62	3.26	1.18	
Ru(0001)	0.00	top_{Cu}	−0.65			1.86	1.86	1.16	1988
		fcc_{Cu_3}	−0.58			1.41	2.09	1.18	1829
		hcp_{Cu_3}	−0.58			1.41	2.09	1.18	1830
	0.25	top_{Pd}	−1.04	1.92	1.92			1.16	2003
		top_{Cu}	−0.58			1.87	1.87	1.16	1987
		hcp_{Cu_2Pd}	−0.77	1.34	2.06	1.47	2.13	1.18	
	1.00	top_{Pd}	−0.79	1.91	1.91			1.16	1999
		fcc_{Pd_3}	−0.98	1.44	2.13			1.18	1824
		hcp_{Pd_3}	−1.03	1.39	2.11			1.19	1828

TABLE III: The CO adsorption properties on close packed Cu-Pd overlayer surfaces. The calculations of $x = 0$ on Cu(111) and $x = 1$ on Pd(111) are found in Table I.

lattice constant is 0.3 Å smaller than the one of Pd.

In order to rationalize these results, we have plotted the corresponding CO adsorption energies as a function of the d-band center in Fig. 5. For the adsorption at the Pd top sites, there is indeed a strong correlation between d-band centers and CO adsorption energies, as has already been found for other CuPd system before [18]. For increasing Pd concentration, the d-band width increases due to the larger overlap. This increase is not caused by the stronger hybridization between the Pd orbitals since in fact the Pd-Cu interaction is stronger than the Pd-Pd interaction [29], but rather by the effective compressive strain for an increasing concentration of the larger metal atom. Consequently, upon increasing Pd concentration, the d-band center shifts down and the CO binding becomes weaker.

For the Cu top sites, for some alloys there seems to be a linear relationship between the Cu d-band center and the CO adsorption energies, but Cu(111), $CuPd_2$/Pd(111) and Cu_2Pd/Pd(111) do not follow this trend. In fact, it has already been observed that adsorption energies on Cu surfaces do not necessarily follow the trends predicted by the d-band model [63, 64], as already mentioned above in the discussion of the results for the bulk alloy surfaces. It has been speculated that this breakdown of the d-band model might be due to the important role of the s-electrons in Cu [63] or due to the strong perturbation of the d states upon adsorption at the top sites [64]. Still the model of the effective compressive strain seems to be operative at the Cu top sites in spite of the fact that it is not fully reflected in the position of the d-band centers.

Recently, the adsorption and desorption of CO on monolayer Cu-Pd surface alloys on Ru(0001) were studied for different compositions using temperature programmed desorption (TPD) and infrared reflection absorption spectroscopy [14]. Therefore we have also calculated CO adsorption energies at the top sites of a Cu monolayer and a Cu_3Pd monolayer surface alloy on Ru(0001) (diamond symbols in Fig. 4a). The trends in the adsorption energies at the top sites of the PdCu/Ru(0001) as a function of the Pd concentration are the same as for the other considered surface alloys. The calculated bulk nearest-neighbor distance in Ru is 2.73 Å, which is intermediate between the values for Cu, 2.61 Å, and Pd, 2.82 Å. Thus, on Ru the lateral compression of the monolayer films is weaker than on Cu and stronger than on Pd. And indeed, the calculated CO adsorption energies on the considered overlayers on the Ru substrate are also intermediate between the results for the Cu substrate and the Pd substrate, indicating that the strain has a decisive influence on the adsorption energies. These findings are thus in agreement with the predictions of the d-band model and also with the experimental findings [14]. Furthermore, our calculations also confirm the experimentally deduced dececreasing stability of the Pd-CO bond at the Pd top sites with increasing Pd concentration of PdCu/Ru(0001).

The trend in the adsorption energies at the most favorable adsorption sites as a function of Pd concentration in Fig. 4b, on the other hand, can easily be understood in terms of the availability of higher coordinated Pd binding sites: CO prefers high coordinated Pd sites so that the adsorption site is changed from Cu top to Pd top, bridge and fcc hollow once such sites become available. Although the single Pd atoms become less reactive for increasing Pd concentration in the surface alloys, the higher coordination overcompensates the reduction in the reactivity. The change in the adsorption sites has also been observed in experiments for PdCu surface alloys on Ru(0001) using IR spectroscopy [14]. The peaks assigned to the Pd hollow and bridge sites vanished at low Pd densities, whereas the peak assigned to the top site became more pronounced.

On the bulk alloys, the adsorption energies are intermediate between the surface alloys on Cu(111) and Pd(111), but the trend is very similar to the surface alloys on Pd(111). Only on Cu(111), the stronger compression accompanying the increasing Pd concentration approximately cancels the coordination effect according to our calculations. In fact, a similar weak dependence of the maximum adsorption energies on the PdCu composition has also been found in the TPD experiments for PdCu surface alloys on Ru(0001) [14].

Finally, we discuss the trends in the CO stretch frequency on the alloy surfaces. Experimentally, CO molecules adsorbed on Cu multilayers on various substrates exhibit a clear correlation between substrate strain and CO stretch frequencies: compressed Cu layers show a red-shift while expanded Cu layers show a blue-shift [69]. In particular, on Cu/Pd(110) the stretch frequency is blue-shifted by 58 cm^{-1} compared to clean Cu(110) [69]. In contrast, in our calculations the CO stretch frequencies on the expanded Cu monolayer on Pd(111) are basically the same as on the clean Cu(111) surface (compare Tables I and III).

For a Cu monolayer on Ru(0001), however, experimentally hardly any shift in the stretch frequency compared to Cu(111) has been observed [14], whereas the calculations yield a red-shift of 15 cm^{-1}. On the Pd monolayer on Ru(0001) a blue-shift of about 10 cm^{-1} compared to Pd(111) has been found [14] while we find again a red-shift in the order of 15 cm^{-1} at the top site but a blue-shift of more than 30 cm^{-1} at the three-fold hollow sites. This red-shift at the top site is indeed surprising considering the lower CO binding energies on Pd/Ru(0001) compared to Pd(111). Probably

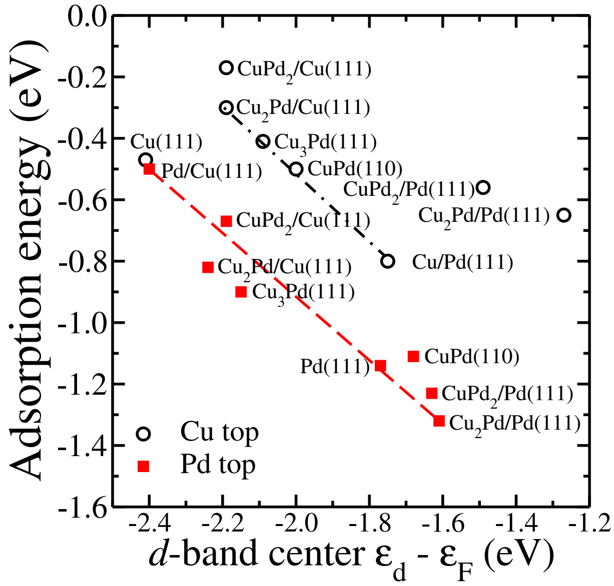

FIG. 5: CO adsorption energies at the top Cu and Pd sites as a function of the *d*-band center at various PdCu alloy surfaces. The lines are plotted as a guide to the eye.

second-layer effects as already obtained for the top sites of Pd/Au [70] and Pt/Au [71] contribute to this difference between top and three-fold hollow sites. Furthermore, the results might also be influenced by the underestimation of the CO HOMO-LUMO gap in the exchange-correlation functional used in this study (see section II). Therefore this point certainly deserves further theoretical studies.

On Pd/Cu(111) we find a red-shift of 8 cm^{-1} at the top site, but a strong blue-shift of 73 cm^{-1} at the three-fold hollow sites, compared to Pd(111). As far as the surface alloys are concerned, there is no clear correlation between CO stretch frequency, Pd concentration and CO adsorption energy. At the Pd top sites, the changes are below 5 cm^{-1} for the surface alloys on Pd(111) and Cu(111) and somewhat larger for the one considered surface alloy on Ru(0001), compared to pure Pd(111). Experimentally, there is a relatively weak dependence of the CO stretch frequency at the top sites of the PdCu/Ru(0001) surface alloys on the composition of the overlayer [14], as confirmed by our calculations, in spite of the calculated changes in the adsorption energies of up to 0.3 eV.

IV. CONCLUSION

The influence of electronic ligand effects versus geometric ensemble effects on the CO adsorption properties on Cu-Pd alloy surfaces has been investigated theoretically by performing electronic structure calculations using density functional theory within the generalized gradient approximation for the exchange correlation effects. For most adsorption properties we find intermediate values between those of pure Pd and Cu caused by the strong interaction between Pd and Cu. However, for the pseudomorphic surface alloys on Cu(111), Pd(111) and Ru(0001) we find that the reactivity of the single Pd and Cu atoms decreases with increasing concentration of the more reactive metal, Pd, which is demonstrated by the decreasing CO binding energies at the top sites. This ligand effect, that has also been found experimentally for PdCu/Ru(0001) alloys, is caused by the effective compressive strain induced by the larger Pd atom. For the Pd sites, this trend in the reactivity is reflected in a corresponding shift of the d-band center, whereas for the Cu sites there is no clear correlation between d-band center and interaction strength.

On the other hand, the binding energies at the most favorable adsorption sites rise for higher Pd concentration. This is caused by an ensemble effect, namely the availability of higher coordinated Pd sites: the most stable configuration is changed from the Pd top site at low Pd density via the Pd bridge position to the threefold-hollow Pd site at high Pd concentration. At the surfaces of the bulk alloys, the trends in the adsorption energy as a function of the Pd concentration are less clear because of the absence of effective strain effects. In spite of the change of the adsorption energies, the stretch frequency of CO adsorbed on the top sites is hardly influenced by the composition of the surface alloy and strain effects, in contrast to the Pd threefold hollow sites where large blue-shifts for the compressed Pd layers on Cu(111) and Ru(0001) have been obtained.

Acknowledgements

This work has been supported by the German Science Foundation (DFG) within the Priority Program 1091 (project GR1503/12-2).

[1] Rodriguez, J. A. *Surf. Sci. Rep.* **1996**, *24*, 223.
[2] Schlögl, R. *Angew. Chem. Int. Ed.* **1998**, *37*, 2333.
[3] Greeley, J.; Gokhale, A. A.; Kreuser, J.; Dumesic, J. A.; Topsøe, H.; Topsøe, N.-Y.; Mavrikakis, M. *J. Catal.* **2003**, *213*, 63–72.
[4] Zambelli, T.; Wintterlin, J.; Trost, J.; Ertl, G. *Science* **1996**, *273*, 1688.
[5] Besenbacher, F.; Chorkendorff, I.; Clausen, B. S.; Hammer, B.; Molenbroek, A. M.; Nørskov, J. K.; Stensgaard, I. *Science* **1998**, *279*, 1913–1915.
[6] Reddington, E.; Sapienza, A.; Gurau, B.; Viswanathan, R.; Sarangapani, S.; Smotkin, E. S.; Mallouk, T. E. *Science* **1998**, *280*, 1735–1737.
[7] Jacobsen, C. J. H.; Dahl, S.; Clausen, B. S.; Bahn, S.; Logadottir, A.; Nørskov, J. K. *J. Am. Chem. Soc.* **2001**, *123*, 8404.
[8] Greeley, J.; Mavrikakis, M. *Nature Mat.* **2004**, *3*, 810.
[9] Groß, A. *Top. Catal.* **2006**, *37*, 29.
[10] Fernández-García, M.; Martínez-Arias, A.; Belver, C.; Anderson, J.; Conesa, J.; Soria, J. *J. Catal.* **2000**, *190*, 387–395.
[11] Deubage, Y.; Abon, M.; Bertolini, J.; Massardier, J.; Rochefort, A. *Appl. Surf. Sci.* **1995**, *90*, 15.
[12] Stamenković, V. R.; Arenz, M.; Lucas, C. A.; Gallagher, M. E.; Ross, P. N.; Marković, N. M. *J. Am. Chem. Soc.* **2003**, *125*, 2736.
[13] Andersen, T. H.; Bech, L.; Li, Z.; Hoffmann, S. V.; Onsgaard, J. *Surf. Sci.* **2004**, *559*, 111.
[14] Hager, T.; Rauscher, H.; Behm, R. J. *Surf. Sci.* **2004**, *558*, 181–194.
[15] Hammer, B.; Morikawa, Y.; Nørskov, J. K. *Phys. Rev. Lett.* **1996**, *76*, 2141.
[16] Ge, Q.; Desai, S.; Neurock, M.; Kourtakis, K. *J. Phys. Chem. B* **2001**, *105*, 9533–9536.
[17] Liu, P.; Nørskov, J. K. *Phys. Chem. Chem. Phys.* **2001**, *3*, 3814–3818.
[18] Lopez, N.; Nørskov, J. K. *Surf. Sci.* **2001**, *477*, 59.
[19] Koper, M.; Shubina, T.; van Santen, R. A. *J. Phys. Chem. B* **2002**, *106*, 686.
[20] Schlapka, A.; Lischka, M.; Groß, A.; Käsberger, U.; Jakob, P. *Phys. Rev. Lett.* **2003**, *91*, 016101.
[21] Roudgar, A.; Groß, A. *J. Electroanal. Chem.* **2003**, *548*, 121.
[22] Roudgar, A.; Groß, A. *Surf. Sci.* **2004**, *559*, L180–L186.
[23] Mousa, M. S.; Hammoudeh, A.; Loboda-Cackovic, J.; Block, J. H. *J. Mol. Catal. A: Chem.* **1995**, *96*, 271.
[24] Paglieri, S. N.; Way, J. D. *Sep. Purif. Methods* **2002**, *31*, 1.
[25] Kamakoti, P.; Morreale, B. D.; Ciocco, M. V.; Howard, B. H.; Killmeyer, R. P.; Cugini, A. V.; Sholl, D. S. *Science* **2005**, *307*, 569.
[26] Hammer, B.; Nørskov, J. K. *Surf. Sci.* **1995**, *343*, 211–220.
[27] Mavrikakis, M.; Hammer, B.; Nørskov, J. K. *Phys. Rev. Lett.* **1998**, *81*, 2819.
[28] Illas, F.; López, N.; Ricart, J. M.; Clotet, A.; Conesa, J. C.; Fernández-García, M. *J. Phys. Chem. B* **1998**, *102*, 8017.
[29] Roudgar, A.; Groß, A. *Surf. Sci.* **2005**, *597*, 42.
[30] Kresse, G.; Furthmüller, J. *Comput. Mater. Sci.* **1996**, *6*, 15–50.
[31] Perdew, J. P.; Chevary, J. A.; Vosko, S. H.; Jackson, K. A.; Pederson, M. R.; Singh, D. J.; Fiolhais, C. *Phys. Rev. B* **1992**, *46*, 6671.
[32] Perdew, J. P.; Burke, K.; Ernzerhof, M. *Phys. Rev. Lett.* **1996**, *77*, 3865.
[33] Hammer, B.; Hansen, L. B.; Nørskov, J. K. *Phys. Rev. B* **1999**, *59*, 7413.
[34] Blöchl, P. *Phys. Rev. B* **1994**, *50*, 17953–17979.
[35] Kresse, G.; Joubert, D. *Phys. Rev. B* **1999**, *59*, 1758.
[36] Huber, K. P.; Herzberg, G. *Molecular Spectra and Molecular Structure*, Vol. IV. Constants of Diatomic Molecules; Van Nostrand Reinhold, New York, 1979.
[37] Baro, A.; Ibach, H. *J. Chem. Phys.* **1979**, *71*, 4812.
[38] Steininger, H.; Lehwald, S.; Ibach, H. *Surf. Sci.* **1982**, *123*, 264.
[39] Hollins, P.; Pritchard, J. *Surf. Sci.* **1979**, *89*, 486–495.
[40] Kirstein, W.; Krüger, B.; Thieme, F. *Surf. Sci.* **1986**,

176, 505.
[41] Bönicke, I.; Kirstein, W.; Spinzig, S.; Thieme, F. *Surf. Sci.* **1994**, *313*, 231–238.
[42] Kneitz, S.; Gemeinhardt, J.; Steinrück, H.-P. *Surf. Sci.* **1999**, *440*, 307–320.
[43] Feibelman, P. J.; Hammer, B.; Nørskov, J. K.; Wagner, F.; Scheffler, M.; Stumpf, R.; Watwe, R.; Dumesic, J. *J. Phys. Chem. B* **2001**, *105*, 4018.
[44] Gil, A.; Clotet, A.; Ricart, J. M.; Kresse, G.; García-Hernández, M.; Rösch, N.; Sautet, P. *Surf. Sci.* **2003**, *530*, 71.
[45] Grinberg, I.; Yourdshahyan, Y.; Rappe, A. M. *J. Chem. Phys.* **2002**, *117*, 2264.
[46] Kresse, G.; Gil, A.; Sautet, P. *Phys. Rev. B* **2003**, *68*, 073401.
[47] Köhler, L.; Kresse, G. *Phys. Rev. B* **2004**, *70*, 165405.
[48] Gajdoš, M.; Eichler, A.; Hafner, J.; Meyer, G.; Rieder, K.-H. *Phys. Rev. B* **2005**, *71*, 035402.
[49] Dudarev, S. L.; Botton, G. A.; Savrasov, S. Y.; Humphreys, C. J.; Sutton, A. P. *Phys. Rev. B* **1998**, *57*, 1505.
[50] Moler, E. J.; Kellar, S. A.; Huff, W. R. A.; Hussain, Z.; Chen, Y.; Shirley, D. A. *Phys. Rev. B* **1996**, *54*, 10862–10868.
[51] Surnev, S.; Sock, M.; Ramsey, M. G.; Netzer, F. P.; Wiklund, M.; Borg, M.; Andersen, J. N. *Surf. Sci.* **2000**, *470*, 171.
[52] Gießel, T.; Schaff, O.; Hirschmugl, C.; Fernandez, V.; Schindler, K.-M.; Theobald, A.; Bao, S.; Lindsay, R.; Berndt, W.; Bradshaw, A.; Baddeley, C.; Lee, A.; Lambert, R.; Woodruff, D. *Surf. Sci.* **1998**, *406*, 90.
[53] Sautet, P.; Rose, M.; Dunphy, J.; Behler, S.; Salmeron, M. *Surf. Sci.* **2000**, *453*, 25.
[54] Guo, X.; Yates Jr., J. T. *J. Chem. Phys.* **1989**, *90*, 6761.
[55] Bradshaw, A. M.; Hoffmann, F. M. *Surf. Sci.* **1978**, *72*, 513–535.
[56] Blyholder, G. *J. Phys. Chem.* **1964**, *68*, 2772.
[57] Lischka, M.; Mosch, C.; Groß, A. *Electrochim. Acta, accepted for publication.*
[58] Mårtensson, N.; Nyholm, R.; Calén, H.; Hedman, J. *Phys. Rev. B* **1981**, *24*, 1725.
[59] Abrikosov, I. A.; Olovsson, W.; Johansson, B. *Phys. Rev. Lett.* **2001**, *87*, 176403.
[60] Nahm, T.-U.; Han, M.; Oh, S.-J.; Park, J.-H.; Allen, J. W.; Chung, S.-M. *Phys. Rev. B* **1995**, *51*, 8140.
[61] Nahm, T.-U.; Jung, R.; Kim, J.-Y.; Park, W.-G.; Oh, S.-J.; Park, J.-H.; Allen, J. W.; Chung, S.-M.; Lee, Y. S.; Whang, C. N. *Phys. Rev. B* **1998**, *58*, 9817.
[62] Cho, E.-J.; Lee, S.; Oh, S.-J.; Han, M.; Lee, Y. S.; Whang, C. N. *Phys. Rev. B* **1995**, *52*, 16443.
[63] Šljivančanin, Ž; Hammer, B. *Phys. Rev. B* **2002**, *65*, 85414.
[64] Sakong, S.; Groß, A. *Surf. Sci.* **2003**, *525*, 107–118.
[65] Hammoudeh, A.; Mousa, M.; Loboda-Cackovic, J. *Vacuum* **1999**, *54*, 239.
[66] Ruban, A.; Skriver, H.; Nørskov, J. *Phys. Rev. B* **1999**, *59*, 15990.
[67] Ruban, A.; Hammer, B.; Stoltze, P. Skriver, H. L.; Nørskov, J. K. *J. Mol. Catal. A* **1997**, *115*, 421–429.
[68] Xu, Y.; Mavrikakis, M. *Surf. Sci.* **2001**, *494*, 131–144.
[69] Kampshoff, E.; Hahn, E.; Kern, K. *Phys. Rev. Lett.* **1994**, *73*, 704.
[70] Roudgar, A.; Groß, A. *Phys. Rev. B* **2003**, *67*, 033409.
[71] Gohda, Y.; Groß, A. *J. Electroanal. Chem., accepted for publication.*